TFC modeling of hydrogenated methane premixed combustion

A. Mameri[1*], A. Kaabi[2] and I. Gökalp[3]

[1] Institut des Sciences Technologiques, Centre Universitaire Larbi Ben M'Hidi, Oum El Bouaghi, Algérie
[2] Département du Génie Climatique, Université des Frères Mentouri, Constantine, Algérie
[3] Institut de Combustion, Aérothermique, Réactivité et Environnement, 'ICARE', CNRS, Orléans, France

Abstract - *The use of hydrogenated fuels shows considerable promise for applications in gas turbines and internal combustion engines. Hydrogen addition to methane will have an important role to reach a fully developed hydrogen economy. The effects of this addition on the flame structure is evaluated in three fuels with the following compositions at constant global equivalent ratio: 100 % CH_4, 10 % H_2 + 90 % CH_4, 20 % H_2 + 80 % CH_4. The turbulence is modeled by the standard k - ε model which is improved by the Pope correction in order to better predict round jet spreading. Combustion is modeled by the turbulent flame closure (TFC) model which is used with flamelet to give detailed chemistry. Computations were achieved by the ANSYS CFX code. A good agreement with experiments was found, it was noted that one can replace a significant fraction of basic fuel by hydrogen without making recourse to major modifications on the installations.*

Résumé - *L'utilisation de combustibles hydrogénés est très prometteuse pour des applications dans les turbines à gaz et les moteurs à combustion interne. L'hydrogène en addition avec le méthane aura un rôle important pour arriver à une économie en hydrogène pleinement développé. Les effets de cet ajout sur la structure de la flamme est évalué à trois carburants à la suite de compositions à taux constant global équivalent: 100 % CH_4, 10 % H_2 + 90 % CH_4, 20 % H_2 + 80 % CH_4. La turbulence est modélisé par le modèle standard k - ε, qui est inspiré par la correction de Pope, afin de mieux prédire la propagation du jet. La combustion est modélisée par le modèle de la fermeture de la flamme turbulente (TFC), qui est utilisé avec des flamelets de façon détaillée en chimie. Les calculs ont été réalisés par le code ANSYS CFX. Un bon accord a été trouvé avec les expériences. Il est à noter que l'on peut remplacer une fraction importante du carburant de base par de l'hydrogène sans recourir à des modifications importantes sur les installations.*

Keywords: Premixed flames - Hydrogenated fuels - Burning velocity - Turbulent flame speed.

1. INTRODUCTION

Internal combustion engine and gas turbine manufacturers are faced with stricter anti-pollution regulations. Lean premixed combustion is a well established technique to achieve low emissions while maintaining high efficiency. According to the thermal NO_X generation mechanism; low flame temperatures given by lean conditions, results in low NO_X emissions. However, close to lean flammability limits, the stability of the flame decreases and flame extinction phenomena may occur.

Since further reduction of NO_X will require even leaner mixtures, schemes for lean stability extension must be considered. A solution to increase the flame stability at lean condition is to add small amounts of hydrogen into the mixtures [1-4]. Several studies

* mameriabdelbaki@yahoo.fr

have been performed to estimate the impact of H_2 addition on the stability, on the reactivity and on the pollutant emissions of the methane-air flames.

It has been shown that hydrogen addition, at constant global equivalence ratio, extends the lean operating limit of natural gas engines, leading to a potential decrease in pollutant formation. The origin of this effect is that the stretch resistance of these flames is considerably increased by hydrogen blending, while other properties are comparatively little modified.

In spark ignited engine [5], the authors show that mixture of natural gas blended with hydrogen improves thermal efficiency, specific fuel consumption, reduces CO and NO_x emissions, extend lean operating limit to lower equivalence ratios and finally allows stable engine operation with lower pollutant emissions.

Hydrogen addition was experimentally tested in several atmospheric flame burners' configurations. It was observed a decreasing in the height of the blue cone with hydrogen addition. The increase in laminar burning velocity was identified as the main effect of the behavior of this parameter. Also a significant reduction in CO emission was obtained [6].

Experimental investigation on the flame stability of hydrogenated mixtures was also performed for swirl stabilized flame configuration [7].

We perform a numerical study to understand and to complete F. Halter *et al.* [8] measured data. The authors conducted experiments on a lean methane combustor at several pressures with hydrogen enrichment.

2. EXPERIMENTAL SETUP

The ICARE (Institut de Combustion, Aérothermique, Réactivité et Environnement) high pressure turbulent flame facility is composed from stainless steel cylindrical combustion chamber (Fig. 1). The inner chamber diameter is 300 mm. The chamber is composed of two superposed vertical portion each of 600 mm height, and each equipped with four windows of 100 mm diameter for optical diagnostics.

Fig. 1: ICARE combustion installation

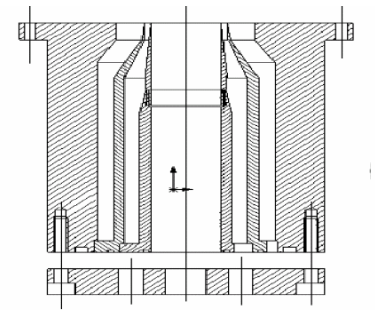

Fig. 2: Bunsen burner

An axisymmetric bunsen type turbulent burner (Fig. 2) is located inside the chamber. The burner internal diameter is 25 mm. It is fed by methane/hydrogen/air mixtures.

The global equivalence ratio is 0.6, the bulk mean flow velocity of the reactants, at the exit is 2 m/s. The reactants flow exhibits a turbulence level about 10 %. The integral length scale is about 3 mm.

3. COMPUTATIONAL MODEL

To gain a more complete understanding of the impact of H_2 addition to lean CH_4 flames, the Ansys CFX 11 code is used to compute the multi component turbulent reacting flow. The Reynolds averaged equations are given by:

Continuity

$$\frac{\partial \rho}{\partial t} + \nabla \bullet (\rho U) = 0 \tag{1}$$

Momentum

$$\frac{\partial \rho U}{\partial t} + \nabla \bullet \{\rho (U \otimes U)\} = \nabla \bullet (\tau - \overline{\rho u' \otimes u'}) + S_M \tag{2}$$

Energy

$$\frac{\partial \rho h_{tot}}{\partial t} - \frac{\partial p}{\partial t} + \nabla \bullet \rho (U h_{tot}) = \nabla \bullet (\lambda \nabla T - \overline{\rho u' h'}) + S_h \tag{3}$$

Where $h_{tot} = h + \frac{1}{2} U^2 + k$

The other equations are similar and they can be cast in the following general form:

$$\frac{\partial \rho \phi}{\partial t} + \nabla \bullet \rho (U \phi) = \nabla \bullet (\Gamma_\phi \nabla \phi - \overline{\rho u' \phi'}) + S_\phi \tag{4}$$

Where ϕ is a general scalar.

The perfect gas state equation is given by:

$$p = \rho R T \sum_j \frac{Y_j}{W_j} \tag{5}$$

The Reynolds stresses $\overline{\rho u' \otimes u'}$ and fluxes $\overline{\rho u' \phi'}$ represent the convective effect of turbulent velocity fluctuations. These terms need to be modelled.

3.1 $k - \varepsilon$ turbulence model

Today, even with the successful development of DNS and LES for turbulent flows, the most popular models for industrial modeling are the two-equation Reynolds averaged Navier-Stokes (RANS) models. Of these, the $k - \varepsilon$ two equations model accounts for 95 % or more of the industrial use at the present [9]. This form of model is easy to solve, converges relatively quickly, is numerically robust and stable, is able to solve large domains and high Reynolds numbers and requires minimal computational expense, which is important for industrial models. The standard $k - \varepsilon$ model with the standard constants predicts the velocity field of a two dimensional plane jet quite accurately, but results in large errors for axisymmetric round jets. Although the standard $k - \varepsilon$ model matches the spreading rate of the round jet more accurately than other two equations models, it still overestimates it by 15 % [10]. In this model, the Reynolds stresses are given by a Newtonian type closure which looks like:

$$-\overline{\rho u' \otimes u'} = \mu_t (\nabla.U + (\nabla.U)^T) - \frac{2}{3}\delta(\rho k + \mu_t \nabla.U) \quad (6)$$

Where μ_t is the turbulence 'viscosity' (also called the eddy viscosity). By analogy with the turbulence viscosity, the turbulence diffusivity is defined, and the Reynolds fluxes are given by:

$$-\overline{\rho u' \phi'} = \Gamma_t . \nabla . \phi \quad (7)$$

Where Γ_t is the turbulence 'diffusivity', it is related to the turbulence viscosity by:

$$\Gamma_t = \frac{\mu_t}{Pr_t} \quad (8)$$

Where Pr_t is the turbulent Prandtl number.

In the $k-\varepsilon$ model, the turbulent viscosity is computed by the relation:

$$\mu_t = C_\mu . \rho . \frac{k^2}{\varepsilon} \quad (9)$$

The k and ε equations are given by:

$$\frac{\partial \rho k}{\partial t} + \nabla \bullet \rho (U k) = \nabla \bullet \left[\left(\mu + \frac{\mu_t}{\sigma_k} \right) . \nabla k \right] + P_k - \rho \varepsilon \quad (10)$$

$$\frac{\partial \rho \varepsilon}{\partial t} + \nabla \bullet \rho (U \varepsilon) = \nabla \bullet \left[\left(\mu + \frac{\mu_t}{\sigma_\varepsilon} \right) . \nabla \varepsilon \right] + \frac{\varepsilon}{k} . \left(C_{\varepsilon 1} P_k - C_{\varepsilon 2} \rho \varepsilon \right) \quad (11)$$

To tailor the $k-\varepsilon$ model for solving round jet flows, McGuirk and Rodi [11], Morse [12], Launder *et al.* [13], and Pope [10] suggested modified turbulence model constants. The best correction in our case is the Pope's one; it is a new source term added to the ε equation. It is given by the following relation:

$$S_{pope} = C_{\varepsilon 3} . \rho . \frac{\varepsilon^2}{k} . \chi_p \quad (12)$$

With

$$\chi_p = \frac{1}{4} \left(\frac{k}{\varepsilon} \right)^3 . \left(\frac{\partial u}{\partial y} - \frac{\partial v}{\partial x} \right)^2 . \left(\frac{\partial u}{\partial x} - \frac{\partial v}{\partial y} \right) \quad (13)$$

for two dimensional axisymmetric geometry.

In this work, a limited version of the Pope correction introduced by Davidenko [14] is adopted and incorporated in the CFX code. Its expression is:

$$S_{pope} = C_{\varepsilon 3} . \rho . \frac{\varepsilon^2}{k} . \min \left(\left| \chi_p \right|, \chi_{lim} \right) sign(\chi_p) \quad (14)$$

With χ_{lim}, a limiting value of χ_p.

3.2 Combustion model

The model for premixed or partially premixed combustion can be split into two independent parts:

• Model for the progress of the global reaction: Burning Velocity Model (BVM), also called Turbulent Flame Closure (TFC);

• Model for the composition of the reacted and non-reacted fractions of the fluid: Laminar Flamelet with PDF.

Reaction Progress

A single progress variable $\widetilde{c}$ is used to describe the progress of the global reaction:

$$\widetilde{Y}_i = (1-\widetilde{c}).\widetilde{Y}_{ifresh} + \widetilde{c}.\widetilde{Y}_{iburnd} \tag{15}$$

The reaction progress variable is computed by solving a transport equation:

$$\frac{\partial \overline{\rho}\,\widetilde{c}}{\partial t} + \frac{\partial (\overline{\rho}\,\widetilde{u}_i\,\widetilde{c})}{\partial x_j} = \frac{\partial}{\partial x_j}\left[\left(\overline{\rho}.\overline{D} + \frac{\mu_t}{\sigma_c}\right).\frac{\partial \widetilde{c}}{\partial x_j}\right] + \overline{\omega}_c \tag{16}$$

The burning velocity model (BVM), also known as turbulent flame closure (TFC), is used to close the combustion source term for reaction progress.

$$\overline{\omega}_c = \overline{\rho}_u.S_T.\left|\nabla.\widetilde{c}\right| - \frac{\partial}{\partial x_j}\left[\overline{\rho}.\overline{D}.\frac{\partial \widetilde{c}}{\partial x_j}\right] \tag{17}$$

Where the turbulent flame velocity is given by:

$$S_T = A.G.u'^{3/4}.S_L^{1/2}.\lambda_u^{-1/4}.l_t^{1/4} \tag{18}$$

And the stretch factor:

$$G = \frac{1}{2}\mathrm{erfc}\left[-\frac{1}{\sqrt{2\sigma}}.\left(\ln\left(\frac{\varepsilon_{cr}}{\varepsilon}\right) + \frac{\sigma}{2}\right)\right] \tag{19}$$

The integral and Kolmogorov length scales are given by:

$$l_t = \frac{k^{3/2}}{\varepsilon} \quad \text{and} \quad \eta = \frac{v^{3/4}}{\varepsilon^{1/4}}$$

Flamelet libraries

Under flamelet regime hypothesis [15], the species transport equations are simplified to:

$$\rho\frac{\partial Y_k}{\partial t} - \frac{\rho\chi_l}{2Le_k}\frac{\partial^2 Y_k}{\partial Z^2} = \omega_k \tag{20}$$

A detailed chemical mechanism of 64 species and 752 equations was adopted.

The simplified energy equation is:

$$\rho\frac{\partial T}{\partial t} - \frac{\rho\chi_l}{2}\frac{\partial^2 T}{\partial Z^2} = \frac{1}{C_p}.\sum_{k=1}^{N} h_k.\omega_k \tag{21}$$

With the laminar scalar dissipation:

$$\chi_l = 2D.(\nabla Z)^2 \tag{22}$$

An external program CFXRIF solves these equations to obtain a laminar flamelet table, which is integrated using a beta PDF to have the turbulent flamelet library.

This library provides the mean species mass fractions as functions of mean mixture fraction $\widetilde{Z}$, variance of mixture fraction $\widetilde{Z}''^2$ and turbulent scalar dissipation rate $\widetilde{\chi}$:

$$\widetilde{Y}_i = \widetilde{Y}_i\left(\widetilde{Z}, \widetilde{Z}''^2, \widetilde{\chi}_{st}\right) \tag{23}$$

On the other hand two transport equations are solved in the CFD code, the first gives mixture fraction:

$$\frac{\partial \overline{\rho}\widetilde{Z}}{\partial t} + \frac{\partial(\overline{\rho}\widetilde{u}_j\widetilde{Z})}{\partial x_j} = \frac{\partial}{\partial x_j}\left(\left(\mu + \frac{\mu_t}{\sigma_z}\right)\frac{\partial \widetilde{Z}}{\partial x_j}\right) \tag{24}$$

And the second gives the mixture fraction variance:

$$\frac{\partial \overline{\rho}\widetilde{Z}}{\partial t} + \frac{\partial(\overline{\rho}\widetilde{u}_j\widetilde{Z})}{\partial x_j} = \frac{\partial}{\partial x_j}\left(\left(\mu + \frac{\mu_t}{\sigma_{z''^2}}\right)\frac{\partial \widetilde{Z}''^2}{\partial x_j}\right) + 2\frac{\mu_t}{\sigma_z}\left(\frac{\partial \widetilde{Z}}{\partial x_j}\right)^2 - \overline{\rho}\widetilde{\chi} \tag{25}$$

The turbulent dissipation scalar is modelled by:

$$\widetilde{\chi} = C_\chi \cdot \frac{\widetilde{\varepsilon}}{\widetilde{k}} \cdot \widetilde{Z}''^2 \tag{26}$$

To interpolate species mass fractions from the turbulent flamelet table, the CFD program use the mixture fraction, mixture fraction variance and the turbulent scalar dissipation computed above.

4. FLAME GEOMETRY AND NUMERICAL PROCEDURE

The computational domain is the half of the chamber with 3 degrees thick (Fig. 3). 200 × 300 × 1 grid nodes are taken inside the domain. The grid is refined near walls and in the high gradients regions (Fig. 4). Boundary conditions for the main flame, pilot flame, at wall, exit and symmetry axis are taken from experiments; the most important are shown for the flame in figure 5.

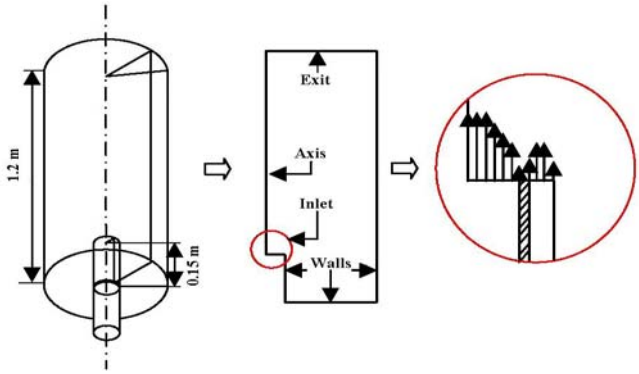

Fig. 3: Combustion chamber geometry

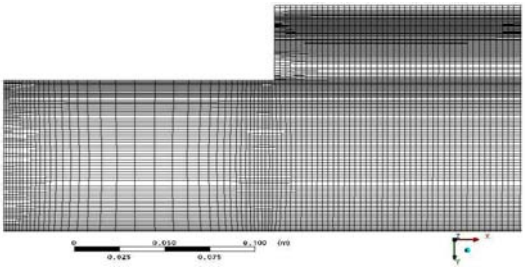

Fig. 4: Near burner meshing

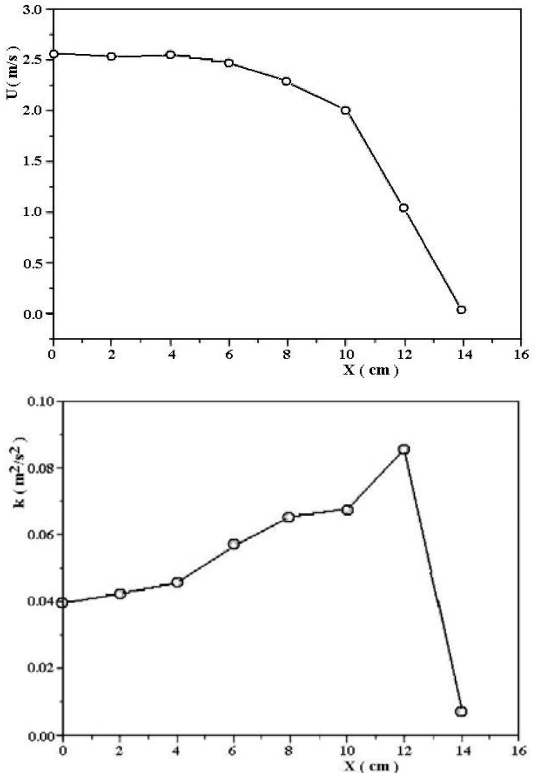

Fig. 5: Inlet velocity and turbulence kinetic energy

A double precision computation is done with the CFX code. The high resolution scheme with an automatic time scale control was used. To reach the target maximum residual of 10^{-7} for all equations, the computation takes about 3000 to 5000 iterations to converge.

5. COMPUTATION RESULTS

5.1 Cold jet test

Before computing the reacting flow, a cold jet test case is performed with the same boundary conditions. The Pope correction constants $C_{\varepsilon 3}$ and χ_{lim} were adjusted to have the best agreement with the experimental axial turbulent kinetic energy variation and mean velocity decay.

The potential core length is well reproduced, the figures 6 and 7 show this agreement. We note that the core length is 75 mm or three times the jet diameter (X / D = 3).

5.2 Reacting flow computations

Three cases are taken into consideration; the first is the methane-air combustion using TFC with a detailed chemical mechanism. The second and third cases are the blended hydrogen-methane combustion using the same model with a chemical

mechanism of 64 species and 752 reactions. The fuel compositions, for the second and third cases, are: 10 % H_2 + 90 % CH_4 and 20 % H_2 + 80 % CH_4.

The following figures showing general field are taken for the case of 10 % H_2. The other cases are similar, and the difference resides in the flame length and maximum variables values. Figure 8 shows the flow structure near the burner. Streamlines are parallel in the potential core, and they are deviated in the preheat zone and the velocity increases under the gas expansion effect.

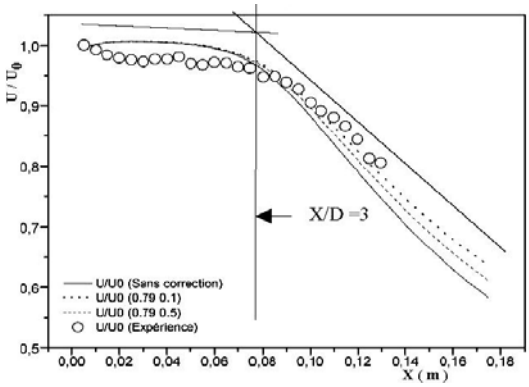

Fig. 6: Axial velocity

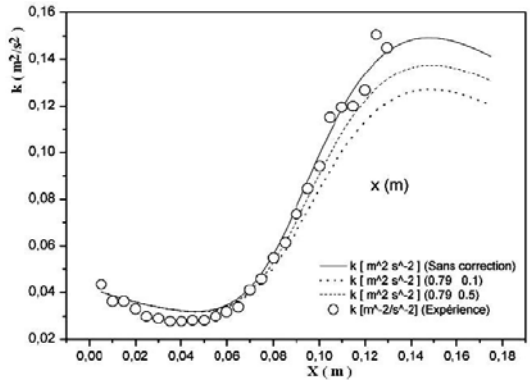

Fig. 7: Axial turbulent kinetic energy

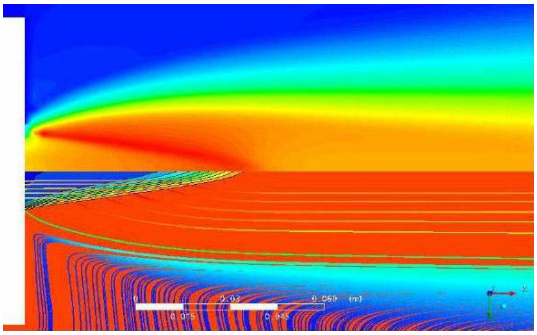

Fig. 8: Near burner flow field

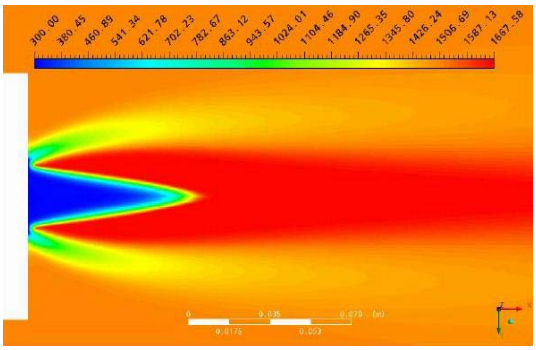

Fig. 9: Near burner temperature field

In figure 9, we have the temperature distribution for the fuel with 10 % H_2. In this case, the maximum temperature is about 1668 K (the adiabatic one is 1674 K). For the case of the pure methane, we obtain 1664 K which is the same as the adiabatic one. The last fuel (20 % H_2) has an adiabatic temperature of 1680 K.

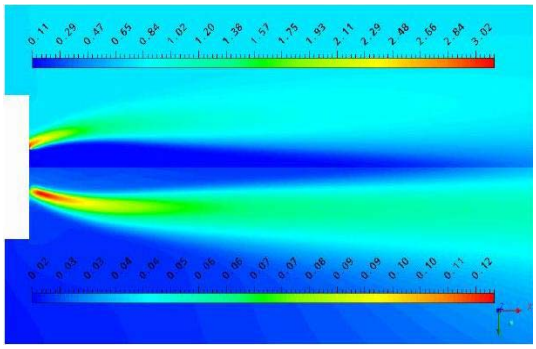

Fig. 10: Top- Turbulent flame velocity; Bottom- Laminar flame velocity

The figure 10 shows the difference between laminar and turbulent flame velocity. The laminar flame velocity is a fuel property; it depends only on the chemical composition. The turbulent flame velocity depends also on the flow conditions. It represents the interaction of the flame with the turbulence. In this case, it is nearly thirty times the laminar one.

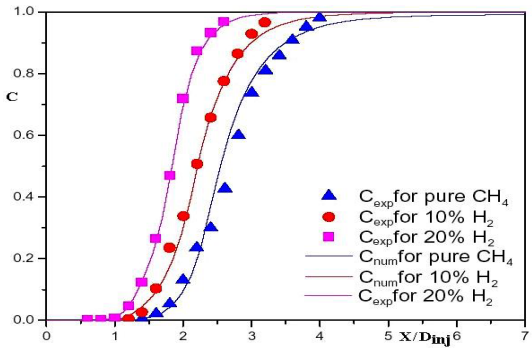

Fig. 11: Axial reaction progress

We can see the good agreement between measured and computed axial reaction progress variable *c* for all fuels (Fig. 11). We note that maximum reaction depends on fuel composition, it becomes close to the burner when we add more hydrogen to the fuel. This means that flame velocity becomes more important.

6. CONCLUSION

In this study turbulent premixed combustion of pure methane and hydrogenated methane is computed. We have used a detailed chemistry with a turbulent flame closure model. The most important result found is that hydrogen enrichment with small amounts doesn't increase significantly combustion temperature. On the other hand it increases flame velocity and stabilises combustion process. Also hydrogen doesn't contain carbon, it is a clean fuel. The replacement of a fraction of the methane by hydrogen results in lower pollutant emissions. Turbine gas and IC engines can be fed with hydrogenated fuels without recourse to major modification in installations.

NOMENCLATURE

A : Zimont model constant

$C_{\varepsilon 2}$: $k-\varepsilon$ model coefficient (= 1.92)

$C_{\varepsilon 1}$: $k-\varepsilon$ model coefficient (= 1.44)

C_{μ} : $k-\varepsilon$ model coefficient (= 0.09)

$C_{\varepsilon 3}$: POPE correction coefficient (= 0.79)

I : Chemical species I

h , h_{tot} : Static and total enthalpy

N_k : Number of species in the mixture

k : Turbulence kinetic energy

R_k : Production rate of species k

Pr_t :Turbulent Prandtl number

S_I : Source term of the I species equation

S_M , S_E : Source terms of the momentum and energy equations

R : Universal gas constant

t : Time

U : Velocity vector $U(u, v, w)$

T : Static temperature

u : Axial velocity component

v : Radial velocity component

W_I : Species I molar weight

Y_i : Species I mass fraction

Greek symbols

α : Hydrogen mass fraction

Γ_t : Turbulent diffusivity coefficient

δ : Kronecker delta

σ_c : Transport coefficient for c (=0.9)

σ : Standard deviation – Distribution of ε

μ : Dynamic viscosity

σ_k , σ_ε : Transport coefficient for k and ε (= 1.0 and 1.3)

σ_Z , $\sigma_{Z''}$: Transport coefficient for $\widetilde{Z}$ and $\widetilde{Z}''^2$ (= 0.9 and 0.9)

μ_t : Turbulent viscosity

ω_c : Rate of production of c

ω_k : Rate of production of species k

χ_p , χ_{lim} : Vortex stretching rate invariant and limited invariant (Pope correction)

REFERENCES

[1] I. Yamaoka and H. Tsuji, '*An Anomalous Behavior of Methane–Air and Methane–Hydrogen–Air Flames Diluted with Nitrogen in a Stagnation Flow*', Process of the Energy Combustion Science, Vol. 24, pp. 145 – 52, 1992.

[2] I. Wierzba and B.B. Ale, '*Rich Flammability Limits of Fuel Mixtures Involving Hydrogen at Elevated Temperatures*', International Journal of Hydrogen Energy, Vol. 25, pp. 75 – 80, 2000.

[3] G.S. Jackson, R. Sai, J.M. Plaia, C.M. Boggs and K.T. Kiger, '*Influence of H_2 on the Response of Lean Premixed CH_4 Flames to High Strained Flows*', Combustion Flame, Vol. 132, pp. 503 – 511, 2003.

[4] A. Mameri, I. Gökalp et D. Boukeffa, '*Simulation Numérique de la Stabilisation d'une Flamme Turbulente de Méthane en Régime Pauvre par Ajout d'Hydrogène*', Revue des Energies Renouvelables, Vol. 10, N°1, pp. 39 – 48, 2007.

[5] S.R. Bell and M. Gupta, '*Extension of the Lean Operating Limit for Natural Gas Fueling of a Spark Ignited Engine Using Hydrogen Blending*', Combustion Science and Technology, Vol. 123, pp. 23 – 48, , 1997.

[6] H.J. Burbano, A.A. Amell and J.M. Garcıa, '*Effects of Hydrogen Addition to Methane on the Flame Structure and CO Emissions in Atmospheric Burners*', International Journal of Hydrogen Energy, Vol. 33, pp. 3410 – 3415, 2008.

[7] R.W. Schefer, '*Combustion of Hydrogen-Enriched Methane in a Lean Premixed Swirl Burner*', In: Proceedings of the 2001 U.S. DOE Hydrogen Program Review, NREL/CP-570-30535, 2001.

[8] F. Halter, C. Chauveau and I. Gökalp, '*Characterization of the Effects of Hydrogen Addition in Premixed Methane/Air Flames*', International Journal of Hydrogen Energy, Vol. 32, pp. 2585 – 2592, 2007.

[9] W.K. George, H. Wang, C. Wollblad and T.G. Tohansson, 14th AFMC, Adelaide, Australia, pp. 41 – 48, 2001.

[10] S.B. Pope, AIAA Journal, Vol. 16, pp. 3, 1978.

[11] J.J. McGuirk and W. Rodi, 1st Symposium on Turbulent Shear Flows, Eds. F. Durst, B.E. Launder, F.W. Schmidt and J.H. Whitelaw, pp. 79 – 83, 1979.

[12] A.P. Morse, Ph.D. Thesis, London University, 1977.

[13] B.E. Launder, A.P. Morse, W. Rodi and D.B. Spalding, Report NASA SP-311, 1972.

[14] D. Davidenko, Ph.D. Thesis, Orleans University, 2005.

[15] N. Peters, '*Turbulent Combustion*', Edition Cambridge University Press, 2000.

[16] Document of Ansys CFX, '*Combustion Theory, User guide*', 2006.

[17] A. Mameri, I. Fedioun et M. Boumaza, '*Simulation Numérique d'une Flamme d'Hydrogène dans l'Air, Confrontation avec l'Expérience*', Revue des Energies Renouvelables, Vol. 9, N°3, pp. 229 – 236, 2006.